MicroRNA-155 modulates bile duct inflammation by targeting the suppressor of cytokine signaling 1 in biliary atresia

Rui Zhao[1], Rui Dong[1], Yifan Yang[1], Yuqing Wang[1], Jin Ma[2], Jiang Wang[1], Hao Li[1] and Shan Zheng[1]

BACKGROUND: Biliary atresia (BA) is an etiologically perplexing disease, manifested by neonatal cholestasis, repeated cholangitis, and progressive biliary fibrosis. MiR-155 has been implicated to modulate the immune response, which contributes to biliary injury. However, its potential role in the pathogenesis of BA has not been addressed so far.

METHODS: The microRNA changes from BA patients and controls were identified via microarray. The immunomodulatory function of miR-155 was investigated via cell transfection and reporter assay. The lentiviral vector pL-miR-155 inhibitor was transfected into a mouse model to investigate its role in BA.

RESULTS: The expression of miR-155 in livers of BA patients was significantly increased, and an inverse correlation between miR-155 and suppressor of cytokine signaling 1 (SOCS1) was detected. MiR-155 overexpression promoted expressions of major histocompatibility complex (MHC) I, MHC II, Chemokine (C-X-C motif) ligand (CXCL) 9, CXCL10, monocyte chemotactic protein 1, and CXCL1 after IFN-γ stimulation, which could be suppressed by SOCS1 overexpression. Moreover, miR-155 overexpression activated JAK2/STAT3, thus enhancing the pro-inflammatory effect. Downregulating miR-155 reduced the incidence of BA in a rhesus monkey rotavirus-induced BA model.

CONCLUSION: Our results reveal a vital contribution of miR-155 upregulation and consequent SOCS1 downregulation to an immune response triggered via IFN-γ in BA.

Biliary atresia (BA) is the principal cause of cholestasis in infants younger than 3 months. BA has a varying incidence, ranging from 1 in 5,000 live births (Taiwan) to 1 in 18,000 (Europe) and 1 in 12,000 (United States). The pathology of early BA includes absence of patent extrahepatic bile ducts (EHBD) with resulting inflammation and ultimately fibrosis in both the extra- and intrahepatic bile ducts. Patients diagnosed with BA suffer from progressive liver fibrosis and cirrhosis and rarely survive for 2 years without treatment (1) Although the Kasai procedure has been reported to significantly improve the prognosis of BA, most patients still require liver transplantation within their lifetime (2). The etiology and pathogenesis of BA remains largely unknown. A leading hypothesis for the pathogenesis of BA is a virus infection-initiated bile duct injury (possibly prenatal), which is then followed by an exaggerated inflammatory or autoimmune response targeting the bile duct epithelium. This ultimately results in progressive bile duct injury, obliteration, and secondary biliary cirrhosis (3,4).

Gene expression is primarily regulated at a post-transcriptional level by microRNAs (miRNAs), which exert their function by targeting complementary mRNA molecules, thus inhibiting their translation by binding to the 3′ untranslated region (UTR) (5). Many miRNAs have been reported to be differentially expressed in autoimmune diseases and consequently may have a pivotal role in the regulation of both immune responses and autoimmunity. MicroRNA-155 (miR-155) is one of the miRNAs that are maximally implicated in autoimmunity, and it was reported to have a central role in the regulation of the innate immune response via modulation of chemokine and cytokine production (6–8). Moreover, many human autoimmune conditions include the aberrant expression of miR-155 (refs 9–11), which has been associated with the impaired autoimmune development of miR-155-deficient mice (8). Via miRNA microarray, we observed an obvious elevation in miR-155 expression in BA liver. However, the role of miR-155 in BA remains elusive.

In the present study, we utilized human intrahepatic biliary epithelial cells (HIBECs) to identify the suppressor of cytokine signaling 1 (SOCS1) as a target of miR-155. SOCS1 is a tumor suppressor, normally functioning as a negative feedback regulator of both Janus-activated kinase (JAK)/signal transducer and activator of transcription (STAT) signaling (12). Furthermore, we report that overexpression of miR-155 in HIBECs promoted inflammation, activated by IFN-γ through the repression of SOCS1. Finally, we report that the upregulation of miR-155 in BA contributed to post-transcriptional silencing of SOCS1, thus leading to constitutive activation of STAT3 in HIBECs. In summary, these results suggest that miR-155 promotes intrahepatic bile duct inflammation and that it has a central role in BA pathogenesis.

[1]Department of Pediatric Surgery, Children's Hospital of Fudan University, Shanghai, People's Republic of China; [2]Department of Infectious Disease, The Fifth People's Hospital of Shanghai, Fudan University, Shanghai, People's Republic of China. Correspondence: Shan Zheng (szheng@shmu.edu.com)

Received 8 June 2016; accepted 9 December 2016; advance online publication 6 September 2017. doi:10.1038/pr.2017.87

Copyright © 2017 International Pediatric Research Foundation

METHODS

Cell Lines and Patient Specimens

A HIBEC line was purchased from ScienCell Research Laboratories (Carlsbad, CA, USA), while human embryonic kidney (HEK) 293T cells were purchased from the American Type Culture Collection (ATCC, Manassas, VA, USA). Media and sera for cell cultures were used as recommended by the respective provider. For inflammatory stimulation, 10 ng/ml IFN-γ was added to the medium. The HIBEC line exhibited low expression of miR-155; therefore, a recombinant lentivirus vector that overexpressed pL-IRES-GFP-Pri-miR-155 was constructed to establish a stable-transfection HIBEC line, overexpressing miR-155 via Gateway cloning technology (13).

Between November 2007 and December 2012, human liver specimens were obtained from nine BA patients and six patients suffering from liver trauma (as normal controls) at the Children's Hospital of Fudan University. Samples were immediately snap-frozen and stored at − 80 °C. The total RNA was isolated from the livers of 15 patients for miRNA microarray experiments. For real-time PCR, ISH, and western blot experiments, liver samples were collected from 15 different BA patients. The liver samples from patients with liver trauma were also used for normal controls in the ISH test. All patients provided written informed consent and freely participated in the study, which was approved by the Research Ethics Committee of Fudan University.

Vector Construction and Cell Transfection

The miR-155 expression vector pL-IRES-GFP-Pri-miR-155, carrying a 400-bp human BIC sequence driven by a cytomegaovirus promoter, was derived from the pLenti6.3-IRES2-GFP/V5 DEST lentiviral vector (Novobioscience, Shanghai, China). A miR-155 inhibition lentiviral vector pL-miR-155 inhibitor was constructed for animal model transfection. We designed and synthesized 3′ UTR and 3′ UTR-mut (24A → G mutation) sequences of the *SOCS1* gene and added the restriction enzyme sites in the sequences of the 5′ and 3′ ends. PCR was used to splice the oligo into a complete gene according to the gene sequence analysis. The 3′ UTR of the *SOCS1* gene was enzyme-digested via *Spe*I/*Hind*III and subsequently cloned into the pMIR-REPORT vector. All plasmids were verified via sequencing. The pMIR-REPORT-SOCS1 3′ UTR and pMIR/REPORT-SOCS1 3′ UTR-mut (A24G) were constructed and transfected into HIBECs using the Lipofectamine 2000 transfection agent (Invitrogen, Grand Island, NY, USA), closely following the manufacturer's protocol. The plasmid pRL-TK, containing the gene that encodes Renilla luciferase (Promega, Madison, WI, USA), was cotransfected to normalize results. Luciferase activities were measured 24 h after transfection via dual-luciferase reporter assay (Promega). For each variant, three independent transfections were performed.

To establish a stable-transfection HIBEC line with the ability to overexpress miR155, HIBECs (2×10^5 per well) were seeded into six-well cell culture plates, cultured overnight, and then transduced with lentiviral vectors, minimizing the volume of medium. Forty-eight hours subsequent to overexpression of the target gene by lentivirus vectors, stable cell lines were selected with 0.5 mg/ml G418. When finally all of the non-transfected cells had disappeared and the isolated colonies started to appear, we chose the colonies with the highest number of cells for expansion. We utilized a limiting dilution assay to obtain transduced cell clones, expressing GFP. The transfection efficiency of lentivirus vector-transduced HIBECs was identified via fluorescence microscopy, while the miR-155 expression was determined via real-time PCR.

Human SOCS1 coding sequences both with and without its 3′ UTR were cloned into a pIRES2-EGFP vector (obtained from Invitrogen) to construct the two SOCS1 expression vectors pIRES2-EGFP-SOCS1-UTR and pIRES2-EGFP-SOCS1, confirming all of these constructs via DNA sequencing. Transfection of pIRES2-EGFP-SOCS1-UTR and pIRES2-EGFP-SOCS1 was performed via Lipofectamine 2000 according to the manufacturer's protocol.

Establishing a RRV-Induced BA Mouse Model and Transfecting the pL-miR-155 Inhibitor

Newborn Balb/c mice were intraperitoneally injected with RRV (20 μl 10^6 PFU) within 24 h after birth, thus generating a BA mouse model. Pregnant Balb/c mice ($n = 9$) were randomly divided into three groups and all newborn mice were grouped with their respective mothers, resulting in three groups: the miR-155 inhibitor group (RRV+pL-miR-155 inhibitor), the miR-155 inhibitor NC group (RRV+ pL-miR-155 inhibitor normal control), and the mock group (RRV group). The lentiviral vectors that contained either the miR-155 inhibitor or the normal control were then intraperitoneally injected in combination with RRV in both the miR-155 inhibitor and the miR-155 inhibitor NC group. Lentiviral transfection efficiencies were evaluated via real-time PCR and western blotting.

miRNA Expression Profiling

For the miRNA hybridization, we hybridized 100 ng of total RNA on an Agilent 8-15K human miRNA one-color microarray, thus detecting 470 human and 64 viral miRNAs, while closely following the manufacturer's protocol (Agilent Technologies, Santa Clara, CA, USA). Agilent Technology microarrays were utilized to perform all gene expressions. Each miRNA array slide was printed with two completely identical arrays to receive two technical replicates. An Axon GenePix 4000B microarray scanner (Molecular Devices, Sunnyvale, CA, USA) at 100% laser power was used to scan the hybridized miRNA array slides, with a photomultiplier tube setting of 600 nm at 5 mm resolution for probes that were labeled with Alexa Fluor 555 (Invitrogen). Image files were quantified via GenePix Pro 4.0 software (Molecular Devices), producing raw image intensity output files for each array. To validate these microarray results, quantitative PCR TaqMan assays (Applied Biosystems, Grand Island, NY, USA) were performed for all candidate miRNAs.

qRT-PCR and RNA Extraction

We extracted the total RNA from either cells or tissues via the TRIzol reagent (purchased from Invitrogen). We quantified the miR-155 level via qRT-PCR, utilizing TaqMan assay kits (purchased from Applied Biosystems), with U6 small nuclear RNA (snRNA) as the internal normalized reference. We determined SOCS1 mRNA levels with the forward primer 5′-agagcttcgactgcctcttc-3′ and the reverse primer 5′-gatgcgctggcggcacagct-3′, using β-actin as internal reference. We analyzed the qRT-PCR results and then expressed them as relative miRNA or mRNA levels of the cycle threshold (CT) value, which we then converted to a fold change.

Western Blot and microRNA ISH

We collected all cells 48 h after transfection (unless otherwise indicated). We purchased all antibodies for SOCS1 and β-actin from Santa Cruz Biotechnology (Santa Cruz Biotechnology, Dallas, TX, USA), while we purchased the antibodies for phosphorylated (p)-JAK2, STAT3, and p-STAT3 from Cell Signaling Technology (Cell Signaling Technology, Danvers, MA, USA). We purchased the antibodies for major histocompatibility complex I (MHC I), major histocompatibility complex II (MHC II), ICAM-1, Chemokine (C-X-C motif) ligand 9 (CXCL9), Chemokine (C-X-C motif) ligand 10 (CXCL10), monocyte chemotactic protein 1 (MCP-1), chemokine (C-X3-C motif) ligand 1 (CX3CL1), and toll-like receptor 3 (TLR3) from Sigma-Aldrich (Sigma-Aldrich, St Louis, MO, USA). We quantified all band intensities with a Storm 860 Molecular Imager (GE, Fairfield, CT, USA).

We utilized formalin-fixed paraffin-embedded BA and control liver sections for ISH with double digoxigenin-labeled locked nucleic acid probes that were labeled at both the 3′ and the 5′ end. We performed locked nucleic acid ISH on paraffin tissue sections with human miR-155-specific probes according to the manufacturer's protocol (Exiqon, Skelstedet, Vedbaek, Denmark), following previously reported instructions (14). We performed ISH scoring with two independent observers, using conventional bright field

Copyright © 2017 International Pediatric Research Foundation

microscopy, and reviewed differences in interpretation to achieve consensus.

Statistical Analysis

For each qRT-PCR run, we utilized the instrument's default threshold settings to calculate CT, using the comparative CT method ($2^{-\Delta\Delta Ct}$) to calculate changes in mRNA expression. We measured protein expression via relative amounts of β-actin, expressing all data as means ± SEM. We used ANOVA with the *post hoc t*-test to determine statistically significant differences between groups, and considered a *P*-value below 0.05 as statistically significant. We performed all statistical analyses using the Stata 12.0 package (Stata Corporation; College Station, TX, USA).

RESULTS

Differential Expression of miRNAs of BA Patients vs. Controls

We analyzed liver tissues from nine patients previously diagnosed with BA and those from six control subjects (suffering from liver trauma as normal control) using a miRNA array platform. We selected differentially expressed miRNAs that had a twofold expression difference between their geometrical means in BA patients and those in controls and a statistically significant *P* value (<0.05) via ANOVA statistics. We then applied the Benjamini and Hoechberg correction for reduction of false positives. We found a total of 23 independent microRNAs to be differentially expressed in BA compared to normal controls (**Table 1**). On the basis of over-inflammation of the bile duct in BA, we chose the multifunctional regulator of innate and adaptive immune responses, miR-155, for further study. We validated the hybridization microarray results via TaqMan assays. We found significantly higher expression levels of miR-155 in the livers from patients with BA compared to those of controls (**Figure 1a**).

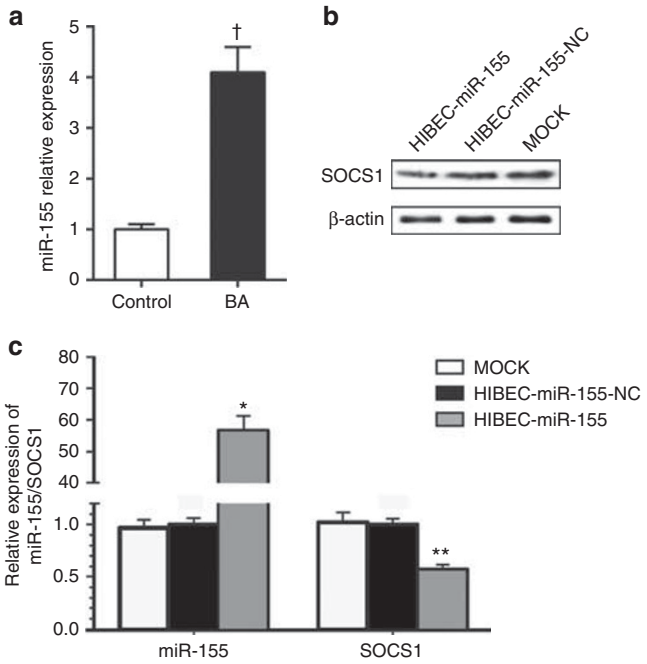

Figure 1. MiR-155 and suppressor of cytokine signaling 1 (SOCS1) mRNA and protein expression in biliary atresia (BA) and human intrahepatic biliary epithelium cell (HIBEC). (**a**) miR-155 expression in the livers of patients with BA was significantly higher than that of controls. (**b**) SOCS1 protein levels were examined via western blot analysis, and β-actin served as an internal reference. SOCS1 protein levels were reduced by 53.6% in HIBECs overexpressing miR-155 compared to controls ($P=0.0211$). Mock group, HIBEC-miR-155-NC group (pL-IRES-GFP), and HIBEC-miR-155 group (pL-IRES-GFP-Pri-miR-155). (**c**) The levels of miR-155 and SOCS1 mRNA were quantified via quantitative reverse transcription-PCR (qRT-PCR) analysis. U6 and β-actin served as internal normalized references for miR-155 and SOCS1 mRNA, respectively. The white, black, and gray columns represent mock, HIBEC-miR-155-NC, and HIBEC-miR-155 groups, respectively. Columns: mean of three separate experiments; bars = SE. $^{\dagger}P=0.003$ vs. control, $^{*}P=0.0004$, $^{**}P=0.008$ vs. mock.

Table 1. Differential expression of miRNAs from BA patients vs. controls

Systematic name	CorrectedPvalue	Log_2fold change	Regulation BA/control	Systematic name	CorrectedPvalue	Log_2fold change	Regulation BA/control
hsa-miR-150	0.002308	1.303	UP	hsa-miR-200a	0.007541	1.121	UP
hsa-miR-342-3p	0.003415	1.156	UP	hsa-miR-376a	0.006352	1.107	UP
hsa-miR-223	0.001201	1.438	UP	hsa-miR-127-3p	0.002774	1.438	UP
hsa-miR-155	0.003012	1.051	UP	hsa-miR-30e	0.002763	−1.271	DOWN
hsa-miR-142-3p	0.004303	1.500	UP	hsa-miR-99a	0.005022	−1.543	DOWN
hsa-miR-494	0.029761	1.243	UP	hsa-miR-30c	0.003762	−1.033	DOWN
hsa-miR-1207-5p	0.005027	1.105	UP	hsa-miR-455-3p	0.047691	−1.215	DOWN
hsa-miR-200b	0.000132	1.987	UP	hsa-miR-122	0.007138	−1.133	DOWN
hsa-miR-34b*	0.016673	1.240	UP	hsa-miR-885-5p	0.005123	−1.275	DOWN
hsa-miR-34a	0.015437	2.695	UP	hsa-miR-574-3p	0.002615	−1.267	DOWN
hsa-miR-21	0.019603	1.635	UP	hsa-miR-483-3p	0.003687	−1.550	DOWN
hsa-miR-410	0.034579	1.199	UP				

Log_2 fold change >1 or <-1 indicates an absolute twofold change upward or downward.

Copyright © 2017 International Pediatric Research Foundation

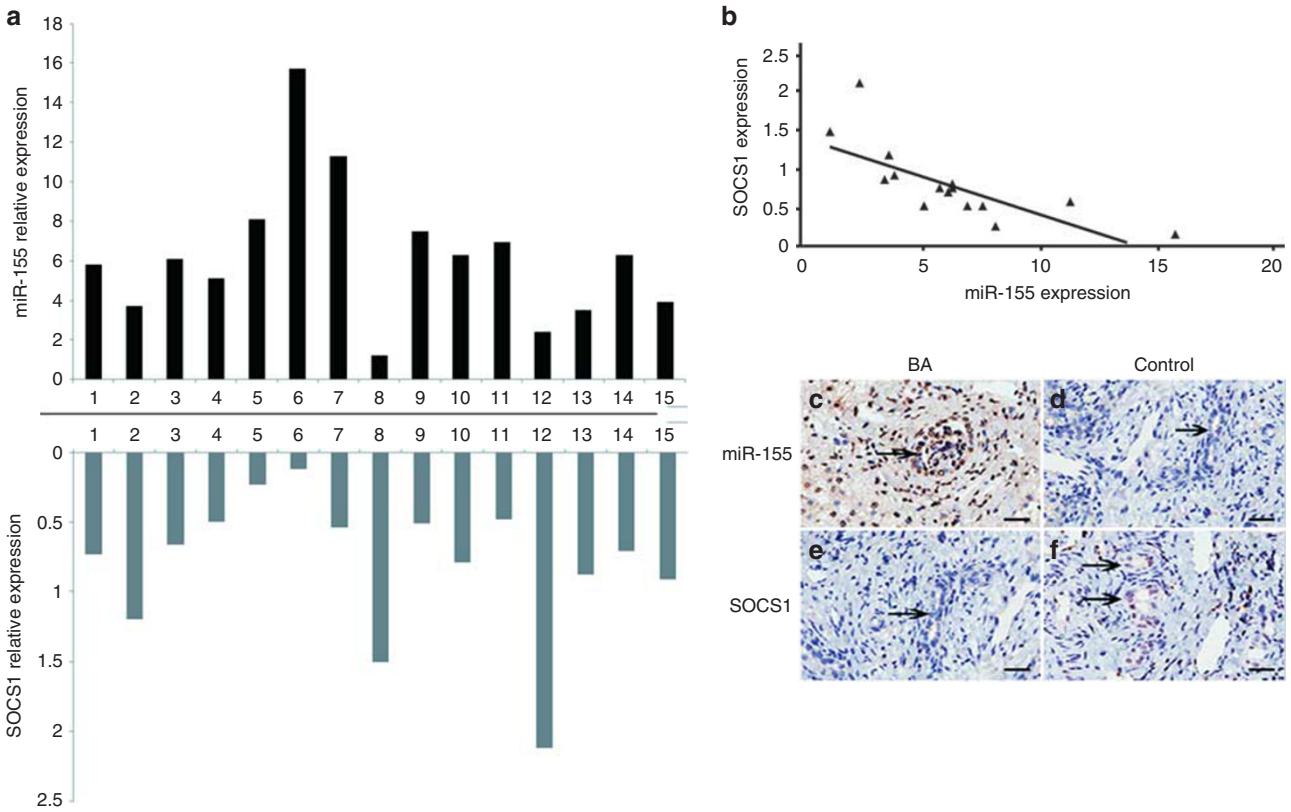

Figure 2. MiR-155 and suppressor of cytokine signaling 1 (SOCS1) mRNA expression in biliary atresia (BA) and control. (**a**) Quantitative reverse transcription-PCR (qRT-PCR) analysis of miR-155 (upper) and SOCS1 (lower) mRNA levels in the liver samples of BA patients. (**b**) indicates a statistically significant inverse correlation ($r = -0.75$, $P = 0.0013$). (**c–f**) miR-155 and SOCS1 expression in the liver samples using in situ hybridization (ISH). miR-155 expression was elevated in BA livers, and was mainly located in the bile duct epithelium (**c**, brown staining) with negative SOCS1 expression (**e**). miR-155 and SOCS1 expression in control livers; negative miR-155 (**d**) and positive SOCS1 expression (**f**, brown staining) in controls. Images have been magnified ×200, bar scale = 40 μm.

Inverse Correlation of miR-155 and SOCS1 Expression in BA

Via computational prediction, we determined SOCS1 to be an evolutionarily conserved target of miR-155. Next, we investigated whether miR-155 overexpression would lead to downregulation of endogenous SOCS1 in BA patients. We specifically overexpressed miR-155 in HIBECs, utilizing a vector construct system. Western blot assays indicated a SOCS1 protein level reduction of 53.6% in HIBECs that overexpressed miR-155, compared to controls (**Figure 1b**). Moreover, quantitative reverse transcription-PCR (qRT-PCR) analyses revealed a downregulated SOCS1 mRNA level by ~43% when miR-155 was overexpressed almost 53-fold (**Figure 1c**). These results reveal SOCS1 to be a direct target of miR-155 in HIBECs and suggest mRNA degradation to be involved in the miR-155-mediated SOCS1 suppression.

To test whether this observation could be extrapolated to BA livers, we examined both SOCS1 and miR-155 expression in 15 liver samples of BA patients. We found that SOCS1 mRNA was reduced to 0.59 ± 0.24 in 12 of the 15 cases and that miR-155 levels were typically elevated in BA livers, while an increase of more than fivefold (6.26 ± 3.6) was found in BA patients (**Figure 2a**). Via Pearson's correlation analysis of socs1-miR-155 expression, we detected a statistically significant inverse correlation ($r = -0.75$, $P = 0.0013$) (**Figure 2b**).

We used miRNA *in situ* hybridization (ISH) of BA livers and normal controls to investigate the location of miR-155 expression. The results showed that miR-155 was mainly expressed in biliary epithelial cells with apparent SOCS1 reduction in BA patients, while we found negative expression of miR-155 and positive expression of SOCS1 in controls (**Figure 2c–f**).

SOCS1 is a Direct Target of miR-155 in HIBEC

To determine whether SOCS1 would be a direct target of miR-155 in HIBECs, we performed a reporter assay using reporter constructs that contain the pMIR-REPORT-SOCS1 3′ UTR and pMIR-REPORT-SOCS1 3′ UTR-mut (A24G). As shown in **Supplementary Figure S1 online**, the pMIR-REPORT-SOCS1–3′-UTR luciferase activity in HIBECs was significantly decreased in the miR-155 mimic group ($P = 0.0005$), while it was significantly increased in the miR-155 inhibitor group ($P = 0.0001$). In contrast, the reporter fused to the A24G-mutated SOCS1 3′ UTR was not repressed by miR-155 ($P > 0.05$), suggesting that the point mutation impairs miR-155 binding to its binding site on the

Copyright © 2017 International Pediatric Research Foundation

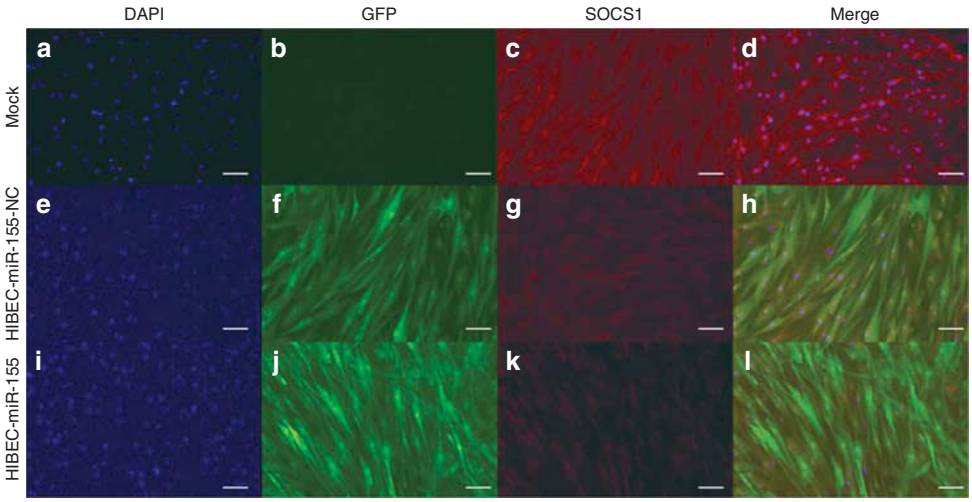

Figure 3. Establishment of the miR-155 stable transfection cell line using the recombinant lentivirus vector overexpressing pL-IRES-GFP-Pri-miR-155. The transfected group at multiplicity of infection = 120 with a transfection efficiency of nearly 93% was observed with fluorescent microscopy with green fluorescent protein (GFP). Immunofluorescence analysis indicated that the suppressor of cytokine signaling 1 (SOCS1) protein level was significantly reduced in human intrahepatic biliary epithelium cells (HIBEC) overexpressing miR-155 compared to controls ($P < 0.05$). (**a**–**d**) The mock group observed with fluorescent microscopy. (**e**–**h**) The HIBEC-miR-155-NC group and (**i**–**l**) the HIBEC-miR-155 group. Blue: nuclei were stained with DAPI. Green: GFP indicated cells with miR-155 expression. Red: SOCS1 protein was immunostained with anti-SOCS1. Images were magnified ×200, bar scale = 40 μm.

SOCS1 3′ UTR and consequently abolishes miR-155 regulation.

miR-155 Promotes the Inflammation Activated by IFN-γ Via Repression of SOCS1 in HIBECs

To imitate the overexpression status of miR-155 in BA, we established a miR-155 stable transfection cell line by utilizing a recombinant lentivirus vector overexpressing pL-IRES-GFP-Pri-miR-155. In our study, we used the green fluorescent protein (GFP)-positive cell ratio to reflect the transduction efficiency of the target gene in HIBECs. Lentiviral vector transduction efficiency of pL-IRES-GFP-Pri-miR-155 was detected via fluorescence microscopy, and was determined to be 93% (**Figure 3**). We verified miR-155 expression in HIBECs via quantitative real-time PCR. The results revealed that miR-155 expression was elevated 53-fold (53.53 ± 3.8). Moreover, immunofluorescence analyses indicated SOCS1 protein levels to be significantly reduced in HIBECs overexpressing miR-155 compared to controls (**Figure 3**).

To determine whether miR-155 promotes the inflammation in HIBEC, we investigated a cluster of cytokines and adhesion molecules in the mock group, the HIBEC-miR-155-NC group, and the HIBEC-miR-155 group. These inflammatory factors, including MHC I, MHC II, ICAM-1, CXCL9, CXCL10, MCP-1, CX3CL1, and TLR3, should be upregulated via IFN-γ stimulation in HIBECs according to published literature (15). In the resting state, hardly any difference could be detected in inflammatory cytokine production between each group (data not shown). However, after IFN-γ stimulation, we found a significant difference: the mRNA and protein expressions of MHC I, MHC II, ICAM-1, CXCL9, CXCL10, MCP-1, and CX3CL1 were sharply increased in the HIBEC-miR-155 group compared to both the mock group and the HIBEC-miR-155-NC group (**Figure 4a**), while TLR3 expression was not significantly altered. These results indicate that overexpression of miR-155 can promote inflammation in HIBECs.

We then performed rescue experiments to further validate that SOCS1 targeting is involved in miR-155-mediated inflammation in HIBECs. We used the two SOCS1 expression vectors, pIRES2-EGFP-SOCS1-UTR and pIRES2-EGFP-SOCS1, in these experiments. Both constructs could similarly overexpress SOCS1 protein in HIBECs with simultaneous low miR-155 expression. Overexpression of the SOCS1 protein greatly suppressed the inflammation of HIBECs overexpressing miR-155 (**Figure 4a**). To our surprise, inclusion of pIRES2-EGFP-SOCS1-UTR in the expression construct significantly attenuated this inhibition (**Figure 4a**). Consistently, cells that were transfected with pIRES2-EGFP-SOCS1 expressed an approximately twofold increase in SOCS1 protein than those transfected with pIRES2-EGFP-SOCS1-UTR (**Figure 4b**). These results suggest that the SOCS1 3′ UTR in the expression vector markedly inhibited the production of SOCS1 protein in miR-155-overexpressing HIBECs.

miR-155 Promotes Inflammation Though the JAK–STAT Signaling Pathway

SOCS1 has previously been reported to negatively regulate cytokine signaling through inhibition of STAT3 via the JAK pathway (16,17). Given that SOCS1 has been detected to be repressed by miR-155, we speculated that miR-155 overexpression in BA may have a central role in JAK–STAT

Copyright © 2017 International Pediatric Research Foundation

signaling. Overexpression of miR-155 in HIBECs resulted in levels of SOCS1 protein that were decreased by 70.5% and increased levels of p-JAK2 and p-STAT3 by ~5.9- and 2.3-fold, respectively (Figure 5a). Furthermore, we used the highly selective and potent JAK2 inhibitor AG490 to validate miR-155-SOCS1–STAT3 axis functionality. As shown in

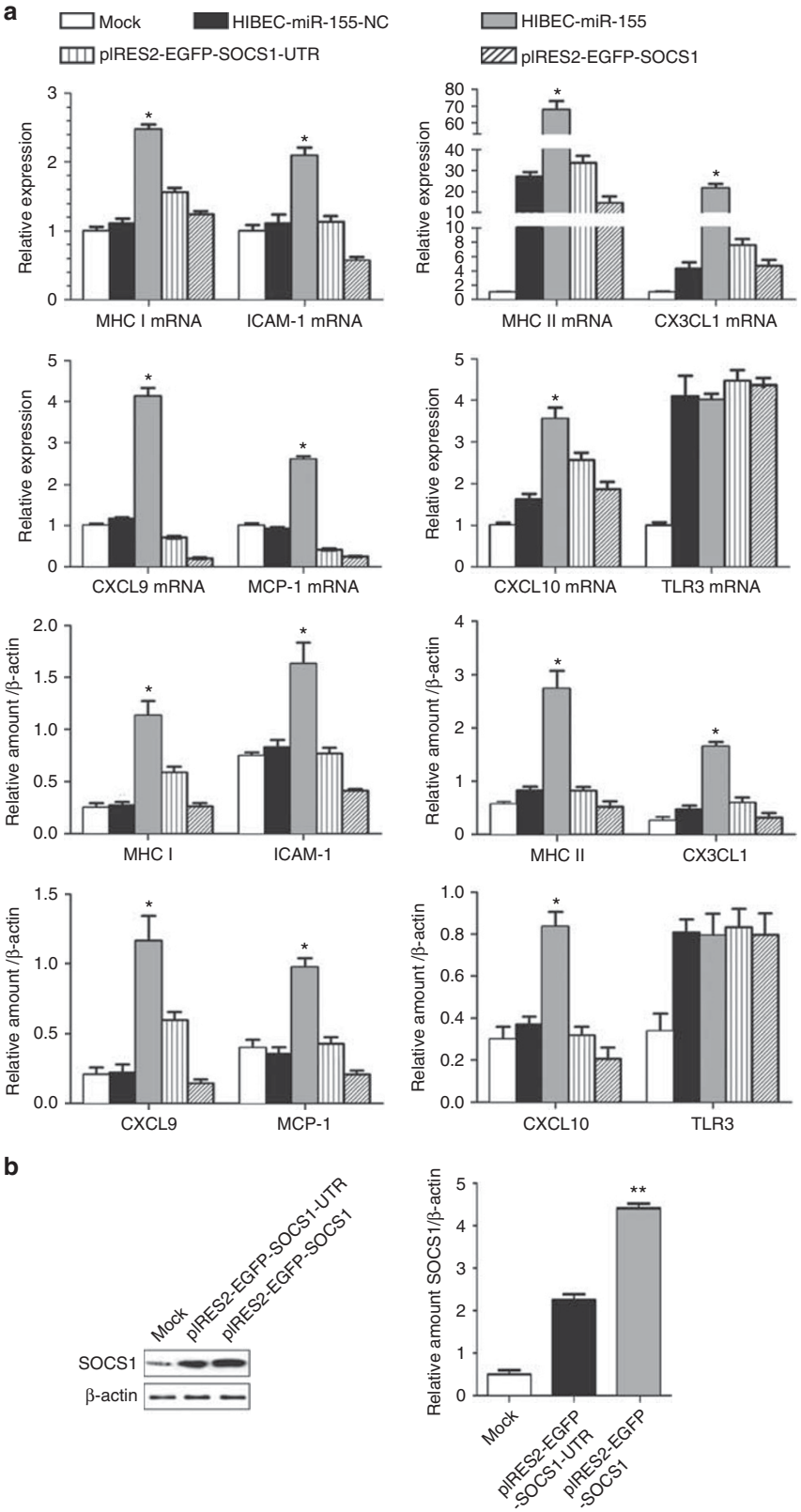

Copyright © 2017 International Pediatric Research Foundation

Figure 5b, miR-155 clearly activated STAT3 with a high level of p-STAT3 in HIBECs, and AG490 reversed the activation of STAT3 and thus the pro-inflammatory effect promoted by miR-155 (Figure 5c). These results suggest that miR-155 overexpression enhances JAK–STAT signaling in HIBECs (Figure 5d).

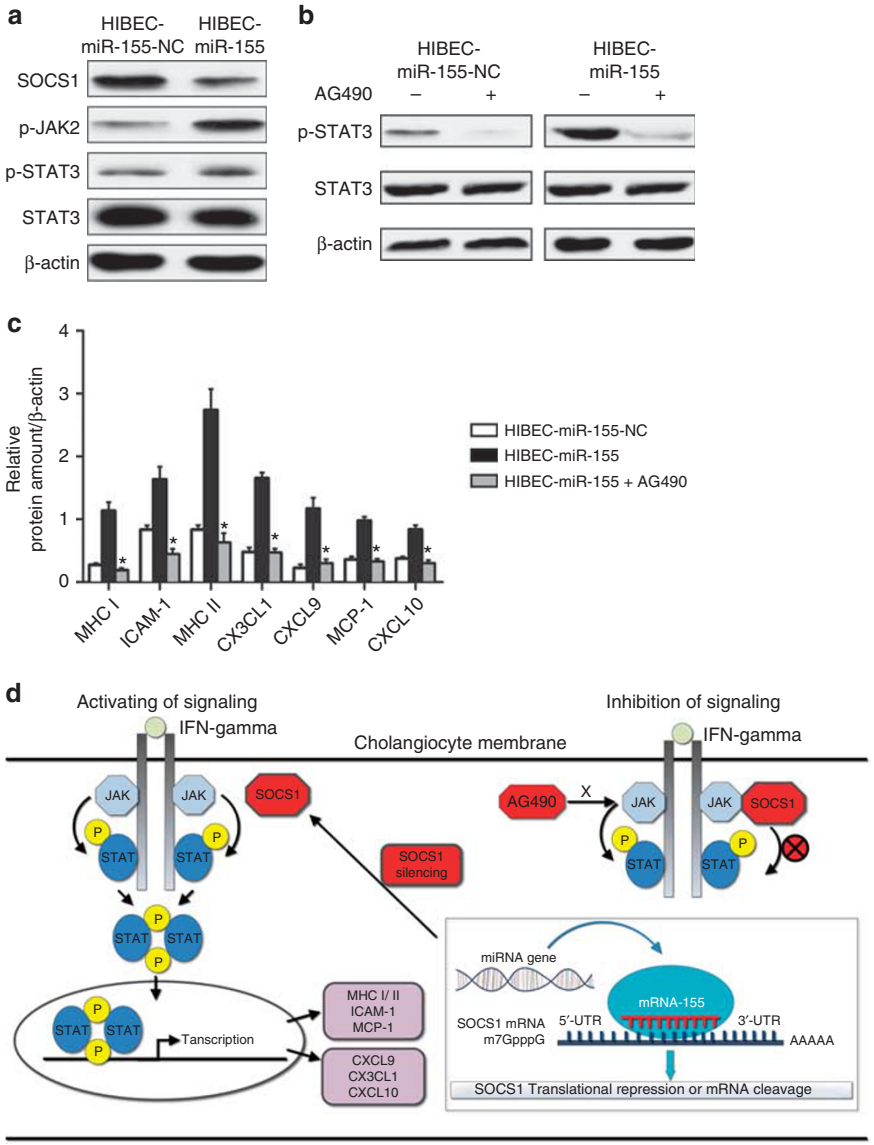

Figure 5. MiR-155 promotes inflammation though the JAK–STAT signaling pathway. (**a**) miR-155 increased the phosphorylated forms of JAK2/STAT3 in human intrahepatic biliary epithelium cells (HIBEC). Western blot analysis was performed 72 h after transfection. (**b**) The JAK2 inhibitor AG490 reversed miR-155-promoted STAT3 activation with a remarkable decrease in phosphorylated forms of JAK2/STAT3. The HIBECs were treated with 50 μmol/l AG490 (JAK2 inhibitor) for 24 h. (**c**) AG490 treatment reversed miR-155-promoted inflammation in HIBECs. The white, black, and gray columns represent HIBEC-miR-155-NC, HIBEC-miR-155, and HIBEC-miR-155+AG490 groups, respectively. (**d**) The model of miR-155 is a key modulator in the IFN-γ signaling pathway. $^{*}P < 0.05$ vs. HIBEC-miR-155.

Figure 4. MiR-155 promotes the inflammation activated by IFN-γ via repression of suppressor of cytokine signaling 1 (SOCS1) in human intrahepatic biliary epithelium cells (HIBEC). (**a**) mRNA and protein expressions of major histocompatibility complex I (MHC I) and ICAM-1, MHC II and CX3CL1, CXCL9 and MCP-1, and CXCL10 and TLR3 are shown. With respect to MHC I, CXCL10, ICAM-1, MHC II, CX3CL1, CXCL9, MCP-1, and CXCL10, miRNA-155 promotes inflammation in HIBECs. Overexpression of SOCS1 protein suppressed the inflammation of HIBECs overexpressing miR-155, and this inhibition was significantly attenuated when the pIRES2-EGFP-SOCS1-UTR was included. However, TLR3 expression revealed no significant changes. The white, black, gray, vertical bar, and slash columns represent mock, HIBEC-miR-155-NC, HIBEC-miR-155, pIRES2-EGFP-SOCS1-UTR, and pIRES2-EGFP-SOCS1 groups, respectively. (**b**) The SOCS1 protein expression in the pIRES2-EGFP-SOCS1-UTR group and the pIRES2-EGFP-SOCS1 group. $^{*}P < 0.05$ vs. HIBEC-miR-155-NC, $^{**}P = 0.0047$ vs. pIRES2-EGFP-SOCS1-UTR.

Copyright © 2017 International Pediatric Research Foundation

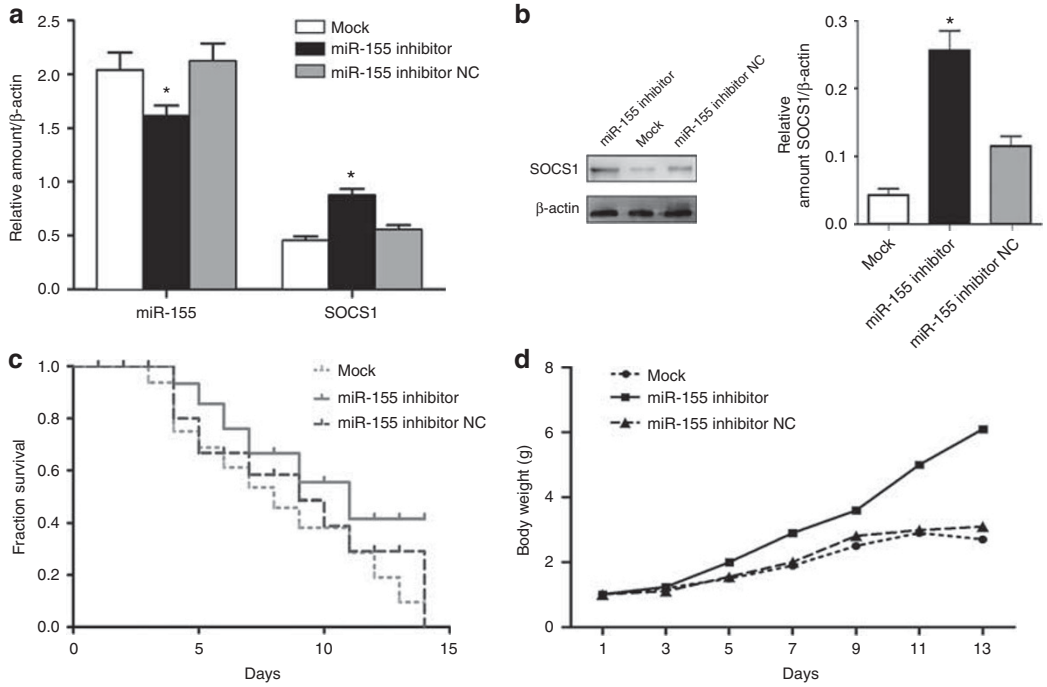

Figure 6. Targeting miR-155 reduced the incidence of biliary atresia (BA) in the rhesus monkey rotavirus (RRV)-induced BA model. (**a**) miR-155 decreased and suppressor of cytokine signaling 1 (SOCS1) mRNA increased after pL-miR-155 inhibitor transfection in the BA model. (**b**) SOCS1 protein increased after pL-miR-155 inhibitor transfection in the BA model via western blot analysis. (**c**) Kaplan–Meier analysis showed that the survival rate in the miR-155 inhibitor group was higher than that in the other two groups; however, no significant difference was observed. (**d**) The growth curve demonstrated that newborn mice benefitted from downregulation of miR-155 in BA mode. *$P<0.05$ vs. miR-155 inhibitor NC.

Targeting miR-155 can Reduce the Incidence of BA in a Rhesus Monkey Rotavirus-Induced BA Model

To study the effects of miR-155 on BA incidence, the lentiviral vector pL-miR-155 inhibitor was constructed and transfected into a rhesus monkey rotavirus (RRV)-induced BA model. miR-155 apparently decreased, while SOCS1 mRNA expression increased, in the miR-155 inhibitor group compared to that in the miR-155 inhibitor NC group and mock group at 14 days after injection (**Figure 6a**). Western blot assays indicated SOCS1 to be elevated in the miR-155 inhibitor group compared to others (**Figure 6b**). These findings indicate that the constructed vector effectively increased SOCS1 via miR-155 expression suppression. Four newborn mice were excluded from the study due to natural death during the first 3 days (1 in the miR-155 inhibitor group, 2 in the miR-155 inhibitor NC group, and 1 in the mock group). BA incidences were 12 out of 19 in the miR-155 inhibitor group, 17 out of 18 in the miR-155 inhibitor NC group, and 16 out of 18 in the mock group. We found significant difference between the miR-155 inhibitor group and the miR-155 inhibitor NC group ($P=0.042$). Kaplan–Meier analysis was conducted for all mice, excluding those killed for specimens and those that died from natural causes during the first 3 days. Although the survival rate in the miR-155 inhibitor group was higher than that in the other two groups, no significant difference was observed (**Figure 6c**). By monitoring the body weight in each group, we found that the newborn mice in the miR-155 inhibitor group grew faster than others (**Figure 6d**). These findings demonstrate that downregulation of miR-155 not only reduced the incidence of BA but also alleviated the symptoms in a RRV-induced BA model.

DISCUSSION

BA is a devastating disease that ultimately leads to cirrhosis and requires liver transplantation in the majority of underage patients. The etiology of BA remains unknown, although a plausible theory suggests the involvement of a primary perinatal hepatobiliary viral infection and the subsequent secondary generation of an autoimmune-mediated bile duct injury. miR-155 has been derived from the non-coding transcript of the proto-oncogene B-cell integration cluster (BIC) gene and represents the only evolutionarily conserved sequence of this gene, suggesting that miR-155 has a central role in BIC function. Similar to other miRNAs, miR-155 binds to the 3′ UTR of mRNA via a protein complex called the RNA-induced silencing complex, thus effecting either mRNA degradation or translational repression. The pivotal role of miR-155 for normal immune function has been highlighted by studies of miR-155-deficient mice. These mice revealed major disturbances in the function of B- and T-lymphocytes. Moreover, miR-155 has also been implicated in numerous autoimmune disorders, such as in rheumatoid arthritis, experimental autoimmune encephalomyelitis (18), and multiple sclerosis. However, miR-155 has not been reported in BA.

Copyright © 2017 International Pediatric Research Foundation

Using a miRNA array, we identified and validated miR-155 overexpression in BA patients. Via miRNA ISH in BA and control liver samples, we found miRNA-155 expression clearly elevated in BA livers, mainly located in the bile duct epithelium. Further investigation demonstrated an inverse correlation of miR-155 and SOCS1 expression in BA, while miR-155 overexpression in HIBECs resulted in a decrease in both *SOCS1* gene and SOCS1 protein expression, indicating SOCS1 as a direct target of miR-155 in HIBECs. Via reporter assay in HIBEC, the A24G mutation was shown to impair miR-155 binding to the miR-155 binding site of SOCS1 3′ UTR, consequently abolishing miR-155 regulation. As a result, this mutation breaks the seventh A–U base pair between the SOCS1 miRNA recognition elements and the miR-155 seed sequences, thus changing a canonical 7-mer A1 seed-matched site to a 6-mer site, which may reduce the efficacy for miRNA target recognition (19,20). Therefore, mutation or loss of miRNA sites in general may be a common mechanism for targets to avoid miRNA repression.

Shivakumar *et al.* (21) demonstrated rhesus rotavirus-infected IFN-γ knockout mice to develop jaundice in a similar way to wild-type controls; however, the cholestasis resolved within 3 weeks of age in 77% of all knockout mice, while the disease progressed in 75% of the wild-type controls. This study strengthened the argument that IFN-γ was responsible for the progression of bile duct injury. IFN-γ relays biological information, thus targeting cells by binding to receptors on the cell surface, consequently activating intracellular signal transduction cascades such as the JAK–STAT pathway. This signaling negatively regulates both magnitude and duration, and the SOCS family of proteins (SOCS1-SOCS7 and CIS) contributes significantly to this process. It is therefore not surprising that miR-155 has a key role in establishing and amplifying inflammatory responses via suppression of SOCS1 in BA.

Growing experimental evidence indicates that cholangiocytes (or biliary epithelial cells) are active players in the immune pathogenesis of both infectious and noninfectious hepatobiliary diseases (such as BA), as they are now known to be immunologically active cells that are central elements in both innate and adaptive immunity. The cytokines secreted by cholangiocytes, in conjunction with the adhesion molecules expressed on their surface, aid the recruitment, localization, and modulation of immune responses in both the liver and the biliary tract (20,21). To determine the pro-inflammatory effect of miR-155, we specifically examined the expression of inflammatory factors that are reported to be upregulated via IFN-γ stimulation in HIBEC. The results revealed that MHC I, MHC II, ICAM-1, CXCL9, CXCL10, MCP-1, and CX3CL1 were sharply increased in the HIBEC-miR-155 group compared to the mock group and the HIBEC-miR-155-NC group. These results indicate that miR-155 overexpression can promote inflammation in HIBECs. That all of these inflammatory factors were reported to be elevated in BA and have been considered to play a role in the pathogenesis of BA (22–24) is rather remarkable. MHC I and ICAM-1 conducted the interaction between T-lymphocytes and cholangiocytes, thus activating cytotoxic T-lymphocytes and causing cholangiocyte injury (25). Cholangiocyte MHC II overexpression has been observed in various injured bile ducts from livers with allograft rejection, graft vs. host disease, primary biliary cirrhosis, and primary biliary cirrhosis. MCP-1 expression is typically upregulated in regenerating bile ducts in pediatric liver diseases (such as BA), and the degree of upregulation has been reported to correlate with disease severity (26). Fractalkine or chemokine (C-X3-C motif) ligand 1 (CX3CL1) is a cytokine of the CX3C family, serving as a chemoattractant and cell adhesion molecule (27). In its soluble form, fractalkine functions as a chemoattractant for T-lymphocytes and monocytes, while fractalkine causes adhesion of leukocytes to cells expressing the CX3CR1 receptor in its cell-bound form (27). Moreover, CXCL9 and CXCL10 were overexpressed in BA models and recruited T-lymphocytes via binding to the CXCR3 receptor (24). These findings suggest that miR-155 amplifies bile duct inflammation triggered by IFN-γ and may have a central role in the pathogenesis of BA.

Moreover, pIRES2-EGFP-SOCS1-UTR and pIRES2-EGFP-SOCS1 were transfected to the miR-155-overexpressing HIBECs. SOCS1 protein overexpression greatly suppressed the inflammation of HIBECs overexpressing miR-155, an inhibition that was significantly attenuated when the pIRES2-EGFP-SOCS1-UTR was included in the expression construct. These findings indicate that the SOCS1 protein reintroduction may override the pro-inflammatory effects of miR-155 overexpression in HIBECs, further suggesting that targeting SOCS1 may be an authentic mechanism by which miR-155 plays its pro-inflammatory role.

Owing to the lack of intrinsic kinase activity of the IFN-γ receptor, it is usually constitutively associated with members of the JAK family of tyrosine kinases. IFN-γ binding leads to receptor aggregation, consequently inducing the juxtaposition of JAKs and activation via cross-phosphorylation. Activated JAKs phosphorylate multiple tyrosine residues of the cytoplasmic domain of cytokine receptors, thus generating recruitment sites for signaling proteins that contain Src-homology 2 or phosphotyrosine binding domains. In this manner, cytokine stimulation initiates multiple signal transduction cascades, ultimately amplifying inflammation (12). Our findings clearly show that miR-155 positively regulates inflammation by targeting SOCS1 via JAK–STAT signaling, and that this process can be suppressed by the selective JAK2 inhibitor AG490.

By targeting miR-155, we reduced the incidence of BA in a RRV-induced BA model. However, complete reversal of BA could not be achieved, the main cause of which might be the transfection efficiency of the lentiviral vector. To obtain a more convincing study, miR-155 knockout Balb/c mice should be investigated in the future. Overall, our results point to an important contribution of miR-155 upregulation, and a resulting SOCS1 downregulation, to the immune response triggered by IFN-γ in BA. Owing to the elevated miR-155

Copyright © 2017 International Pediatric Research Foundation

expression after viral infection, this has been largely associated with the maintenance of a pro-inflammatory phenotype in many autoimmune diseases. Our findings furthermore confirm the hypothesis that BA is initiated by virus infection, followed by an overlarge inflammatory or autoimmune response targeting the bile duct epithelium, leading to progressive bile duct injury and ultimately obliteration. In the light of our results, miR-155 is revealed as an interesting and promising molecular target for the treatment of BA.

SUPPLEMENTARY MATERIAL

Supplementary material is linked to the online version of the paper at http://www.nature.com/pr

STATEMENT OF FINANCIAL SUPPORT

This study received financial support from the National Key Clinical Specialty Construction Programs of China (2014–2016), the Shanghai 'Non Key-in-Key Discipline' Clinical medical centers (2014–2016), the Shanghai Hospital Development Center (SHDC12014106), the Natural Science Foundation of China (Nos. 81200257, 81300517, and 81370472), the Shanghai Hospital Development Center (SHDC12014106), the Shanghai Rising-Star Program (A type) (No. 15QA1400800), and The Science Foundation of Shanghai (No. 16411952200).

Disclosure: The authors declare no conflict of interest.

REFERENCES

1. Mack CL, Feldman AG, Sokol RJ. Clues to the etiology of bile duct injury in biliary atresia. Semin Liver Dis 2012;32:307–16.
2. Davenport M. Biliary atresia: clinical aspects. Semin Pediatr Surg 2012;21:175–84.
3. Mack CL, Sokol RJ. Unraveling the pathogenesis and etiology of biliary atresia. Pediatr Res 2005;57:87R–94R.
4. Bessho K, Bezerra JA. Biliary atresia: will blocking inflammation tame the disease? Annu Rev Med 2011;62:171–85.
5. Baltimore D, Boldin MP, O'Connell RM, Rao DS, Taganov KD. MicroRNAs: new regulators of immune cell development and function. Nat Immunol 2008;9:839–45.
6. Cardoso AL, Guedes JR, Pereira de Almeida L, Pedroso de Lima MC. miR-155 modulates microglia-mediated immune response by down-regulating SOCS-1 and promoting cytokine and nitric oxide production. Immunology 2012;135:73–88.
7. Guedes J, Cardoso AL, Pedroso de Lima MC. Involvement of microRNA in microglia-mediated immune response. Clin Dev Immunol 2013;2013:186872.
8. Thai TH, Calado DP, Casola S, et al. Regulation of the germinal center response by microRNA-155. Science 2007;316:604–8.
9. Wang G, Tam LS, Li EK, et al. Serum and urinary cell-free MiR-146a and MiR-155 in patients with systemic lupus erythematosus. J Rheumatol 2010;37:2516–22.
10. Stanczyk J, Pedrioli DM, Brentano F, et al. Altered expression of MicroRNA in synovial fibroblasts and synovial tissue in rheumatoid arthritis. Arthritis Rheum 2008;58:1001–9.
11. Junker A, Krumbholz M, Eisele S, et al. MicroRNA profiling of multiple sclerosis lesions identifies modulators of the regulatory protein CD47. Brain 2009;132:3342–52.
12. Krebs DL, Hilton DJ. SOCS proteins: negative regulators of cytokine signaling. Stem Cells 2001;19:378–87.
13. Walhout AJ, Temple GF, Brasch MA, et al. GATEWAY recombinational cloning: application to the cloning of large numbers of open reading frames or ORFeomes. Methods Enzymol 2000;328:575–92.
14. Guo Z, Hardin H, Montemayor-Garcia C, et al. *In situ* hybridization analysis of miR-146b-5p and miR-21 in thyroid nodules: diagnostic implications. Endocr Pathol 2015;26:157–63.
15. Syal G, Fausther M, Dranoff JA. Advances in cholangiocyte immunobiology. Am J Physiol Gastrointest Liver Physiol 2012;303:G1077–86.
16. Davey GM, Heath WR, Starr R. SOCS1: a potent and multifaceted regulator of cytokines and cell-mediated inflammation. Tissue Antigens 2006;67:1–9.
17. Jiang S, Zhang HW, Lu MH, et al. MicroRNA-155 functions as an OncomiR in breast cancer by targeting the suppressor of cytokine signaling 1 gene. Cancer Res 2010;70:3119–27.
18. Zhang J, Cheng Y, Cui W, Li M, Li B, Guo L. MicroRNA-155 modulates Th1 and Th17 cell differentiation and is associated with multiple sclerosis and experimental autoimmune encephalomyelitis. J Neuroimmunol 2014;266:56–63.
19. Shukla GC, Singh J, Barik S. MicroRNAs: processing, maturation, target recognition and regulatory functions. Mol Cell Pharmacol 2011;3:83–92.
20. Bartel DP. MicroRNAs: target recognition and regulatory functions. Cell 2009;136:215–33.
21. Shivakumar P, Campbell KM, Sabla GE, et al. Obstruction of extrahepatic bile ducts by lymphocytes is regulated by IFN-gamma in experimental biliary atresia. J Clin Invest 2004;114:322–9.
22. Ayres RC, Neuberger JM, Shaw J, Joplin R, Adams DH. Intercellular adhesion molecule-1 and MHC antigens on human intrahepatic bile duct cells: effect of pro-inflammatory cytokines. Gut 1993;34:1245–9.
23. Chen XM, O'Hara SP, LaRusso NF. The immunobiology of cholangiocytes. Immunol Cell Biol 2008;86:497–505.
24. Al-Masri AN, Flemming P, Rodeck B, Melter M, Leonhardt J, Petersen C. Expression of the interferon-induced Mx proteins in biliary atresia. J Pediatr Surg 2006;41:1139–43.
25. Jafri M, Donnelly B, Bondoc A, Allen S, Tiao G. Cholangiocyte secretion of chemokines in experimental biliary atresia. J Pediatr Surg 2009;44:500–7.
26. Shinkai M, Shinkai T, Puri P, Stringer MD. Increased CXCR3 expression associated with CD3-positive lymphocytes in the liver and biliary remnant in biliary atresia. J Pediatr Surg 2006;41:950–4.
27. Leon MP, Bassendine MF, Gibbs P, Thick M, Kirby JA. Immunogenicity of biliary epithelium: study of the adhesive interaction with lymphocytes. Gastroenterology 1997;112:968–77.
28. Marra F, DeFranco R, Grappone C, et al. Increased expression of monocyte chemotactic protein-1 during active hepatic fibrogenesis: correlation with monocyte infiltration. Am J Pathol 1998;152:423–30.
29. Imai T, Hieshima K, Haskell C, et al. Identification and molecular characterization of fractalkine receptor CX3CR1, which mediates both leukocyte migration and adhesion. Cell 1997;91:521–30.

Copyright © 2017 International Pediatric Research Foundation